Molecular modeling of the inhibitory mechanism of copper(II) on aggregation of amyloid β-peptide

JIAO Yong, HAN Daxiong & YANG Pin

Institute of Molecular Science, Key Laboratory of Chemical Biology and Molecular Engineering of Ministry of Education, Shanxi University, Taiyuan 030006, China
Correspondence should be addressed to Yang Pin (email: yangpin@sxu.edu.cn)

Received May 22, 2005

Abstract Aggregation of amyloid β-peptide (Aβ) into insoluble fibrils is a key pathological event in Alzheimer's disease (AD). Under certain conditions, Cu(II) exhibits strong inhibitory effect on the Zn(II)-induced aggregation, which occurs significantly even at nearly physiological concentrations of zinc ion *in vitro*. Cu(II) is considered as a potential factor in the normal brain preventing Aβ from aggregating. The possible mechanism of the inhibitory effect of Cu(II) is investigated for the first time by molecular modeling method. In the mono-ring mode, the Y10 residue promotes typical quasi-helix conformations of Aβ. Specially, [Cu-H13(Nπ)-Y10(OH)] complex forms a local 3.0_{10} helix conformation. In the multi-ring mode, the side chains of Q15 and E11 residues collaborate harmoniously with other chelating ligands producing markedly low energies and quasi-helix conformations. [Cu-3N-Q15(O)-E11(O1)] and [Cu-H13(Nπ)-Y10(OH)] complex with quasi-helix conformations may prefer soluble forms in solution. In addition, hydrogen-bond interactions may be the main driving force for Aβ aggregation. All the results will provide helpful clues for an improved understanding of the role of Cu(II) in the pathogenesis of AD and contribute to the development of an "anti-amyloid" therapeutic strategy.

Keywords: copper(II), amyloid β-peptide, inhibitory mechanism, Alzheimer's disease, molecular modeling.

DOI: 10.1360/042004-93

Alzheimer's disease (AD) is a devastating form of progressive dementia for which no curative therapies exist. Aggregation of amyloid β-peptide (Aβ) into fibrils is a key pathological event and the hallmark of AD. Considerable experimental data imply that exposure to certain metal ions, such as Zn(II), Al(III) and so on, is a risk factor for developing AD[1–3]. For AD patients, Aβ aggregates and accumulates into the cores which are deposited with numerous associated proteins and other components to form senile plaques, whose extensive deposition causes neurodegeneration[4,5]. Zn(II) rapidly induces Aβ aggregation into insoluble fibrils at physiological concentrations *in vitro*. Recently, we elucidated the binding mode of Zn(II) induced-aggregation, i.e. the insoluble mode, by molecular modeling. Zn(II) associates Aβ by Zn(II)-bridge-bond and plays a crucial role of inducing-core in the assembly of Aβ fibrils. The binding of Zn(II)-Nτ atoms is an important structural factor in driving the aggregating behavior of Aβ and forcefully stabilizes the aggregation[6]. The results suggest that there should exist unclear mechanism preventing Aβ from Zn(II)-induced aggregation in the normal brain, but how does the mechanism operate? Some

recent researches clue us that Cu(II) is involved in this mystery. Cu(II) not only strong inhibits Aβ aggregation under certain conditions but also competes with Zn(II) to inhibit the Zn(II)-induced aggregation. So Cu(II) appeals to many researchers for its potential of being an inhibitor on Aβ aggregation *in vivo*. Recently, it was reported that in severely degenerated brain regions of AD patients such as the amygdala and hippocampus, the concentration of Cu(II) is significantly decreased compared to age-matched controls, however, Zn(II) still remains at comparatively high concentrations[7,8]. These observations suggest that the protective role of Cu(II), i.e. the effective inhibition on the Zn(II)-induced aggregation, is severely weakened by the decrease of Cu(II) concentrations, which results in the excessive deposition of Aβ and the degeneration of the brain.

The inhibitory mechanism of copper(II) on Aβ aggregation was examined by molecular modeling in this work. The interaction of Cu(II)-Aβ was characterized in the soluble binding mode of intramolecular chelation which differed markedly in the insoluble binding mode of intermolecular cross-linking by Zn(II)-bridge-bond. In the mono-ring mode, the Y10 residue promotes quasi-helix conformation of Aβ. Specially, [Cu-H13(Nπ)-Y10(OH)] complex forms a local 3.0_{10} helix conformation. In the multi-ring mode, the side chains of Q15 and E11 residues collaborate harmoniously with other chelating ligands and result in markedly low energy and quasi-helix conformations. [Cu-3N-Q15(O)-E11(O1)] and [Cu-H13(Nπ)-Y10(OH)] complex with quasi-helix conformations may prefer soluble forms in solution. In addition, hydrogen-bond interaction may be the main driving force for Aβ aggregation. All the above will provide helpful clues for an improved understanding of the role of Cu(II) in the pathogenesis of AD and contribute to the development of an "anti-amyloid" therapeutic strategy.

1 Modeling methods

It is the structure of Aβ fibrils that lays the foundation for investigating effects of metal ions on Aβ aggregation. Using a combination of solid-state NMR, electron microscopy, and small angle neutron scattering methods which allowed Aβ fibrils to be studied directly both in solution and in solid state, the three-dimensional (3D) structure model of Aβ10–35 fibrils was proposed by Lynn's group[9]. This 3D model with the cross-β structure character[10] consisted of a lamination of six parallel β-sheets propagating along the fibrils axis. And within the parallel β-sheet the peptide strands oriented themselves perpendicular to the fibrils axis. The strands held roughly 0.5 nm apart within the β-sheet and the β-sheets held roughly 1.0 nm separation between each other within the fibrils. Lynn's model was confirmed by Raman microscopy data which indicated that fibrils from purified amyloid cores were composed of two filaments of 2–4 nm in diameter. And the filament consisting of Aβ strands was characterized by the space periods of 0.48 and 1.06 nm in the directions of parallel and perpendicular to the fibrils axis, respectively[11]. The above researches indicate that Aβ is highly ordered in fibrils, which provides a dependable experimental restriction for constructing the initial model of theoretical calculation.

As in our previous work on the mechanism of Zn(II)-induced Aβ aggregation, Aβ10–21 (^{10}YEVHHQKLVFFA^{21}) was selected as the simplified model of full length Aβ in this work[6]. Aβ10–21 concentrates most of the metal binding sites, such as Y10, H13, H14 etc., of full length Aβ. Small angle neutron scattering study has elucidated that some metal ions play an important role of being inducing-core in the process of Aβ10–21 aggregation and promote forming the typical amyloid fibrils[12]. Meanwhile, the similarity of chemical and physical properties, and the similarity of the aggregating behavior between Aβ10–21 and Aβ10–35 make Lynn's model can be transplanted into the study of Aβ10–21[12].

It has been revealed that the β-pleated conformation of Aβ is the most preferential form for aggregating and is the structural basis of the assembling forces, such as hydrogen-bond, van der Waals interaction and hydrophobic interaction[7–12]. Once the β-pleated conforma-

tion is severely twisted or destroyed, the conditions of forming hydrogen-bond between the main chains of Aβ will disappear. While van der Waals interaction and hydrophobic interaction will be weakened for the disorder of the stretching directions of the side chains of Aβ, which makes Aβ lose the assembling forces and exist in soluble form in solutions. Therefore, as the initial geometry of the interaction of Cu(II)-Aβ, the parallel-β conformation (Φ=–119°, Ψ= +113°) of Aβ10–21 was constructed and used as the structural motif for establishing the experimentally restrained initial structure of the fibrils of four and sixteen strands. For investigating the soluble binding mode of [Cu(II)-Aβ] complex, the following procedure was carried out. First, four strands Aβ spacing in 0.5 nm between each other were aggregated to form a β-pleated sheet by hydrogen-bond between the main chains of Aβ. Then four same β-pleated sheets spacing in 1.0 nm were laminated in parallel to form cuboid filament (see Fig. 1). Lastly, by using the favorable soluble conformations, the control models of Aβ fibrils were built according to Lynn's model for elucidating the inhibitory effect of Cu(II) on the aggregation of Aβ.

The coordination chemistry of Cu(II) is relatively complex. Its coordination numbers can be four, five, or six and the corresponding coordination geometry are planar quadrangle, tetragonal pyramid or distortional octahedron. According to the ligand field theory, the planar quadrangle configuration is the typically basic structure with relatively favorable coordination energy. The fifth and sixth coordinations along the axis are relatively weak and their geometry are usually distorted with uncertain bond parameters[13–15]. Considering the templet effect of metal ions with which the ligand-field effect is correlative, i.e. the comparative rigidity of the coordination geometry of metal ions, the following modeling steps were carried out. First, making use of the assembly effect of the metal templet, we constructed the calculational models with planar quadrangle geometry. Then the initial conformations were optimized under the restrictions of metal templet. ESFF force field and its default parameters were used.

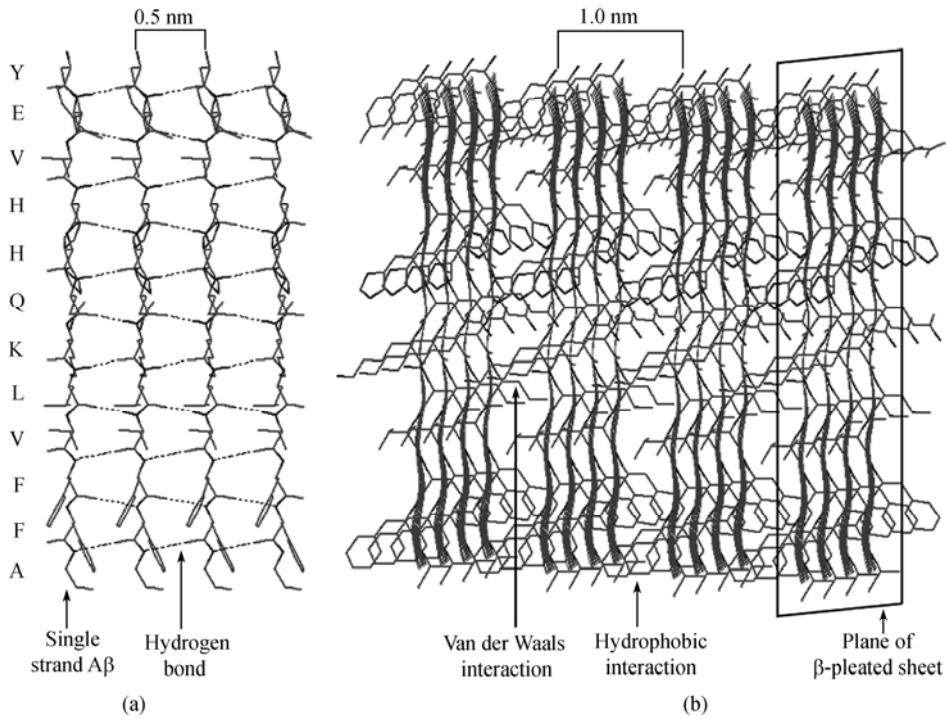

Fig. 1. The structural model of Aβ fibrils. (a) A β-pleated sheet of four strands spacing in 0.5 nm; (b) a filament of four β-pleated sheets spacing in 1.0 nm.

This work was accomplished on SGI workstation with InsightII 2000 software platform.

2 Results and discussion

There are several potential binding sites of metal ions in Aβ10–21, among which the binding affinity of histidine residues is outstandingly strong. Rat Aβ, which contains three amino acid substitutions, R5→G, Y10→F, and H13→R, binds Zn(II) and Cu(II) much less avidly than human Aβ. The ability of metal ions to aggregate human Aβ is diminished by modifying all three histidine residues at positions 6, 13, and 14 with diethyl pyrocarbonate[16]. The reduced affinity of rat Aβ for metal ions is reproduced by the single H13→R mutation of human Aβ. All these observations suggest that the imidazole group of histidine residue has exceeding affinity and is the anchor sites of the interaction between metal ions with Aβ.

Using the imidazole groups of H13 and H14 residues as the anchor sites of Cu(II), the soluble binding mode of [Cu(II)-Aβ] complex was investigated in detail. There are five possible sub-modes of the intramolecular [Cu(II)-Aβ] chelation which are different in the number of chelate rings, i.e. mono-ring, di-ring, tri-ring, tetra-ring and penta-ring sub-modes. The system energy of different sub-modes with the imidazole groups of H13 and H14 residues as the anchor sites of Cu(II) were calculated (see Fig. 2). Fig. 2 shows that the system energy of tri-ring sub-mode is the highest, and mono-ring and penta-ring sub-modes are relatively low. Especially, penta-ring sub-mode in which side chains cooperate with other chelating ligands is the lowest. According to the calculation results, two sub-modes of the soluble binding mode were proposed: (i) mono-ring mode coordinated with water and (ii) multi-ring mode of side chains cooperating mutually.

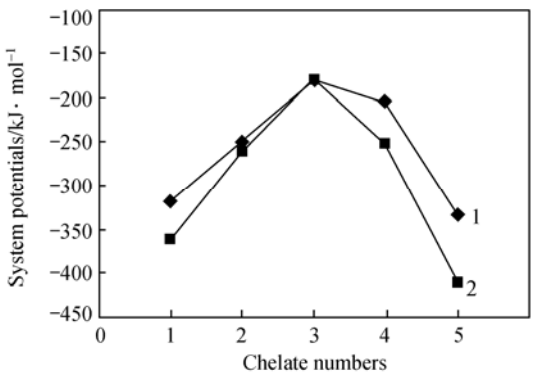

Fig. 2. System potentials of different chelate numbers. 1 and 2 represent the system potentials of different chelate numbers of the anchor sites of H13(Nπ) and H14(Nπ), respectively.

2.1 Mono-ring mode coordinated with water

The mono-ring mode is the simplest mode of intramolecular [Cu(II)-Aβ] chelation restrained in planar quadrangle geometry with the imidazole N atoms of H13 and H14 as the anchor sites. To find the predominant soluble conformations, the calculation of potential energies and the search of conformations of the potential binding sites in the main chain and side chains of Aβ with Cu(II) were performed under the precondition of two water molecules participating in the coordination.

Tables 1 and 2 show that the potential energies of most of the binding sites are relatively low negative values except a very few sites with divergence ener-

Table 1 Potential search of the binding interaction of anchor sites with main-chain atoms (kJ/mol)

Ligand atoms	Anchor sites			
	H13 (Nπ)	H13 (Nτ)	H14 (Nπ)	H14 (Nτ)
Y10(O)	–370.61	–337.21	–373.66	–380.52
Y10(N)	–402.35	–328.76	–370.83	–341.20
E11(O)	–443.38	–369.42	–386.02	–365.02
E11(N)	–333.24	–287.55	–376.61	–291.49
V12(O)	–379.45	–339.62	–430.11	–371.83
V12(N)	–355.55	–282.91	–344.45	–294.44
H13(O)	–348.88	–431.91	–417.54	–343.56
H13(N)	–258.46	–318.24	–354.90	–286.44
H14(O)	–425.32	–353.97	–355.99	–437.05
H14(N)	–337.52	–262.70	–265.70	–361.91
Q15(O)	–360.10	–354.13	–388.26	–363.63
Q15(N)	–364.24	–303.07	–349.72	–267.06
K16(O)	–297.69	–351.85	–407.54	–347.11
K16(N)	–257.46	–285.70	–344.38	–288.88
L17(O)	–410.33	–347.65	–418.39	–338.97
L17(N)	–318.01	–279.04	–358.30	–293.32
V18(O)	–310.90	–373.55	–435.24	–332.77
V18(N)	–335.12	–282.86	–351.57	–278.17
F19(O)	–	–370.83	–344.42	–348.41
F19(N)	–357.40	–290.17	–334.43	–296.54
F20(O)	–385.81	–369.13	–387.32	–363.47
F20(N)	–387.76	–306.65	–364.11	–282.05
A21(O)	–	–316.68	–417.98	–351.82
A21(N)	–385.85	–	–377.01	–280.91

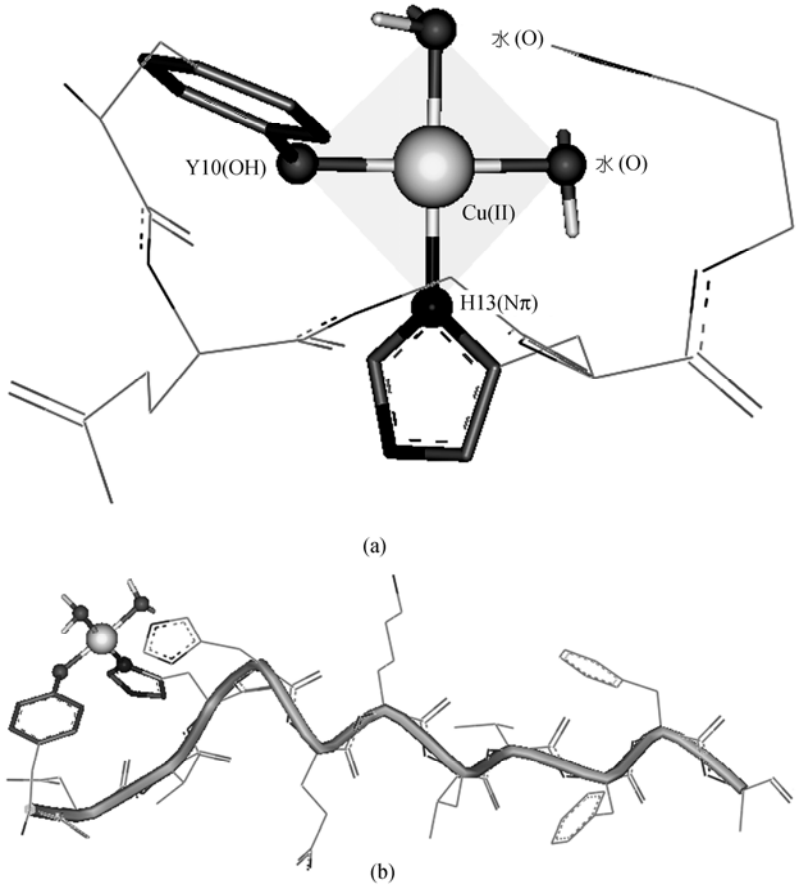

Fig. 3. The effect of promoting helix conformations of Y10. (a) The effect of promoting helix conformations of Y10 in [Cu(II)-H13(Nπ)-Y10(OH)] and (b) in [Cu(II)-H14(Nmain)-Y10(OH)] complex, respectively.

Table 2 Potential search of the binding interaction of anchor sites with side-chain atoms (kJ/mol)

Ligand atoms	Anchor sites			
	H13 (Nπ)	H13 (Nτ)	H14 (Nπ)	H14 (Nτ)
Tyr10-OH	–410.37	–342.56	–370.11	–342.98
Glu11-CO	–449.73	–375.32	–415.20	–377.58
Glu11-OH	–426.42	–355.58	–420.79	–368.34
His13-Nπ	–	–	–378.27	–319.78
His13-N τ	–	–	–311.96	–226.84
His14-Nπ	–346.30	–337.48	–	–
His14-N τ	–328.20	–263.13	–	–
Gln15-CO	–372.13	–385.45	–462.66	–386.16
Gln15-NH	–401.52	–337.53	–376.41	–328.72
Lys16-NH	–401.12	–321.74	–359.97	–322.01

gies. The data indicate that the mono-ring sub-mode stabilizes the [Cu(II)-Aβ] complexes. Meanwhile, the analyses of conformations of the [Cu(II)-Aβ] complexes suggest that the binding of Cu(II) with any site of Aβ always distorts the β conformation to certain extent into quasi-helix or random coil conformations (reported in other paper). Especially, it was found that Y10 residue displays the marked effect of conformational transition on the [Cu(II)-Aβ] complexes. More than 90% quasi-helix conformations exist in the micro-environment with Y10 residue. This indicates that Y10 residue plays an important role of promoting the formation of quasi-helix conformations (Fig. 4). In the [Fe(III)-Aβ] complexes, the coordination affinity of Y10 residue even exceeds that of histidines[17]. The structural characteristics of quasi-helix conformation are as follows: (i) the shrinkage effect of hydrogen bonds, i.e. the extending backbone of Aβ shrinks about 20% of its original length due to forming hydrogen bonds (Fig. 5); (ii) the conformational angles transform from β to helix conformation, resulting in the forming of quasi-helix conformation; (iii) screw-pitch

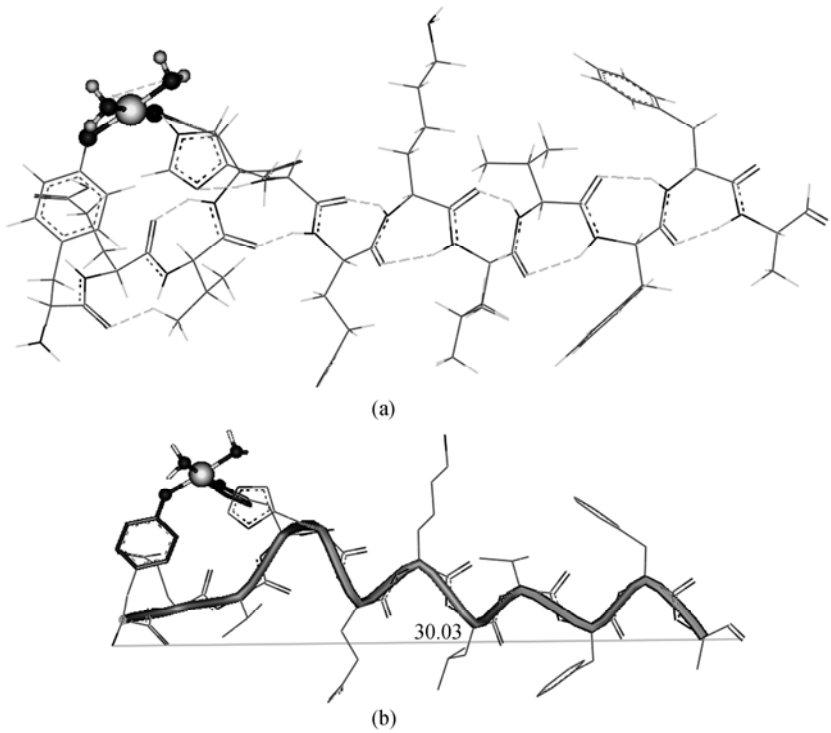

Fig. 4. Formation of intramolecular hydrogen bonds and its shrinkage effect. (a) Formation of 12 intramolecular hydrogen bonds in [Cu-H13(Nπ)-Y10(OH)] complex; (b) the shrinkage effect of hydrogen bonds: the length of peptide chain shrinked from 3.822 to 3.003 nm (30.03 in angstrom was the datum given by the software).

Table 3 The structural parameters of quasi-3.0_{10}-helix conformation in single-ring mode

	Numbers of H-bond	Lengths of main-chain/nm	Atoms in H-bonded loop	Conformational angles		Pitches	Residues per turn
				$\sqrt{}$	Ψ		
[Cu(II)-H13(Nπ)-Y10(OH)]	12	3.003	10	–50.1°	–24.7°	5.9	3.0
3.0_{10}-helix	–	–	10	–49.0°	–26.0°	6.0	3.0
Parallel β-strand	0	3.822	–	–119°	+113°	–	–

and other structural parameters are consistent with that of 3.0_{10} helix. The typical quasi-3.0_{10}-helix conformation was found in [Cu-H13(Nπ)-Y10(OH)] complex (the structural data in Table 3).

2.2 Multi-ring mode in which side chains of Aβ cooperate with each other

Miura inferred from Raman spectra data that the soluble [Cu(II)-Aβ] complex was formed by the tri-ring chelating mode of the Aβ backbone[16]. Cu(II) was coordinated by the Nπ atom of a histidine residue with two or three deprotoned amide nitrogens in the neighborhood. It was found from the calculation of the binding mode of [Zn(II)-Aβ] complex that Miura's tri-ring chelating mode made the system energy significantly increase. So the possibility of the interaction of Zn(II) with Aβ in such mode was excluded[6]. Thanks to the relative rigidity of the coordinating configuration of metal ions, the coordination of metal ions with Aβ will notably distort the Aβ backbone. It is the forming of three chelating rings which tightly borders on each other within three residues in neighborhood that increases the repulsive energy, and the system energy remarkably increases simultaneously. Therefore, Miura's tri-ring mode is not supported by the data of molecular modeling. However, considerable experimental data indicate that the multi-ring chelating mode exists frequently in the interaction of Cu(II) with

peptides (certainly not Aβ)[14,18]. Based on the coordination chemistry of Cu(II) and its coordination geometry found in biological system, we proposed a new multi-ring mode in which side chains cooperate mutually. Considering the flexibility of side chains which makes less structural strain and steric hindrance, we induce two side chains into the tri-ring chelation of the backbone of Aβ with Cu(II) to saturate Cu(II) coordination valences. There are many kinds of dynamically weak interactions in peptide-metal complexes, including stronger long-range coulomb force and weaker short-range dipole-dipole interaction, which cooperate harmoniously and not only compensate the increased energy from the structural distortion but also decrease the system energy significantly. In addition, the chelate effect of five-chelate-ring powerfully stabilizes the soluble conformations in thermodynamics.

The multi-ring mode was modeled as follows. (i) The imidazole Nπ atoms of H13 or H14 residues were used as the anchor sites for Cu(II). The affinity of Cu(II) with histidine residues is stronger than that of Zn(II)[14]. Histidine residues have two types of nitrogen atoms, Nπ and Nτ, both of which can bind with Cu(II). To compare the relative affinity between Nπ and Nτ, the single point binding energies were calculated (see Table 4). The results indicate that the binding energy of Nπ is lower than that of Nτ, so Nπ is prior to binding with Cu(II). Raman spectra indicate that Nπ is prone to forming intramolecular chelation conformation yet Nτ is prone to cross-linking peptides by intermolecular chelation[6]. (ii) The basic coordination configuration of planar quadrangle was created as follows. When nitrogen atoms of histidine residues function as anchor sites, Cu(II) is characterized in promoting deprotonation of main-chain amide nitrogens in the vicinity of the anchor sites[18]. And it is well known that the chelate ring of five or six members displays the marked chelation effect and makes the system more stable. So the basic coordination configuration of planar quadrangle of Cu(II) was constructed by using the deprotonation main-chain nitrogen atoms as the chelate sites and the Nπ atoms of H13 and H14 as anchor sites, respectively. Thus we could make as many of the chelate ring of five or six members as possible. (iii) Based on the basic coordination configuration of planar quadrangle, the atoms of side chains with coordination affinity were used as the fifth and sixth atoms coordinating along the axis of the complex. Thus the coordination valences of Cu(II) were saturated.

Table 4 Potentials of the anchor sites of histidine binding with Cu(II) (kJ/mol)

Histidines	Ligand atoms	Potentials	Remarks
H13	Nπ	–483.6467	anchor 1
	Nτ	–406.8698	–
H14	Nπ	–486.6751	anchor 2
	Nτ	–408.6083	–

The data of fifty conformations of multi-ring mode and their energies were obtained by energy searching (see Fig. 5). The coordination environments were searched systematically by altering the coordination sites which form the fourth and fifth chelate rings. It was found that the lowest energy distribution was centralized in the coordination environments consisting of the side chains of Q15 and E11 residues. Especially, the carbonyl group of Q15 residue was the most favorable coordination site. The side chains with the lower energy always were those of Q15 and E11 no matter whether the anchor site was H13(Nπ) or H14(Nπ). The secondary structure and its coordination environment of [Cu-3N-Q15(O)-E11(O1)] complex, which has the lowest energy, are shown in Fig. 5. The local quasi-helix conformation centralized by Cu(II), the shrinkage effect of hydrogen bonds and the trend of transforming to helix conformation of [Cu-3N-Q15(O)-E11(O1)] complex are shown in Figs. 6 and 7, respectively.

In short, by employing H13(Nπ) and H14(Nπ) as anchor sites and the deprotoned amide nitrogen atoms of the backbone of Aβ as binding sites, Cu(II) creates the basic coordination configuration of planar quadrangle, in which three chelate rings of five or six members exist. And the basic coordination configuration of planar quadrangle cooperates with the side chains of Q15 and E11 residues finishing the construction of the stable soluble conformations of penta-ring mode.

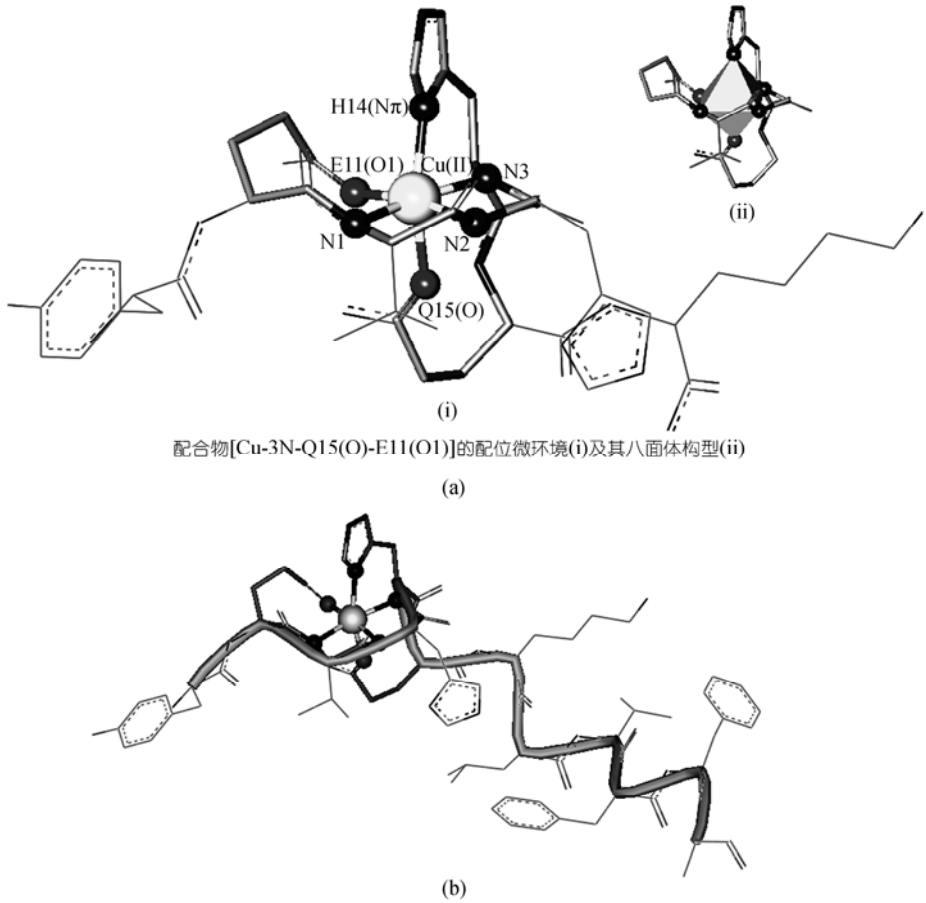

Fig. 5. Coordinating microenvironment and local quasi-helix conformation. (a) Coordinating microenvironment and (b) local quasi-helix conformation of [Cu-3N-Q15(O)-E11(O1)] complex.

Table 5 Potential search of multi-ring mode of taking H13(Nπ)\H14(Nπ) as anchors (kJ/mol) [a)]

Side chain	Y10(O)	E11(O1)	E11(O2)	H13(Nπ)	H13(Nτ)	H14(Nπ)	H14(Nτ)	Q15(O)	Q15(N)	K16(N)
Y10(O)		–303.5	–250.0			–274.3	–225.7	–316.7	–282.8	–287.4
E11(O1)	–326.7					–296.6	–219.7	–335.1	–351.7	–291.6
E11(O2)	–341.1					–306.6	–232.9	–382.1	–334.3	–302.2
H13(Nπ)	–312.9	–325.2	–335.9							
H13(Nτ)	–242.1	–252.6	–236.4							
H14(Nπ)								–338.3	–296.3	–282.0
H14(Nτ)								–273.4	–341.4	–239.9
Q15(O)	–293.6	–410.7	–401.6	–338.4	–267.5					–318.8
Q15(N)	–292.4	–307.2	–335.1	–304.9	–196.4					–299.9
K16(N)	–317.4	–333.2	–333.1	–306.8	–217.7			–290.6	–233.9	

a) The data above the diagonal belong to the anchor of H13(Nπ) and that below the diagonal belong to the anchor of H14(Nπ).

2.3 The comparative study of the driving forces on Aβ aggregation and the stability of aggregating systems

(i) The driving forces on Aβ aggregation. According to the parameters of Lynn's model, the double-strand aggregating system of the standard Aβ spacing 0.5 nm between backbones and the double-strand aggregating system of the distorted penta-ring complex [Cu-3N-Q15(O)-E11(O1)] spacing 1.0 nm between side chains were built by hydrogen bonds interaction and by van der Waals interaction,

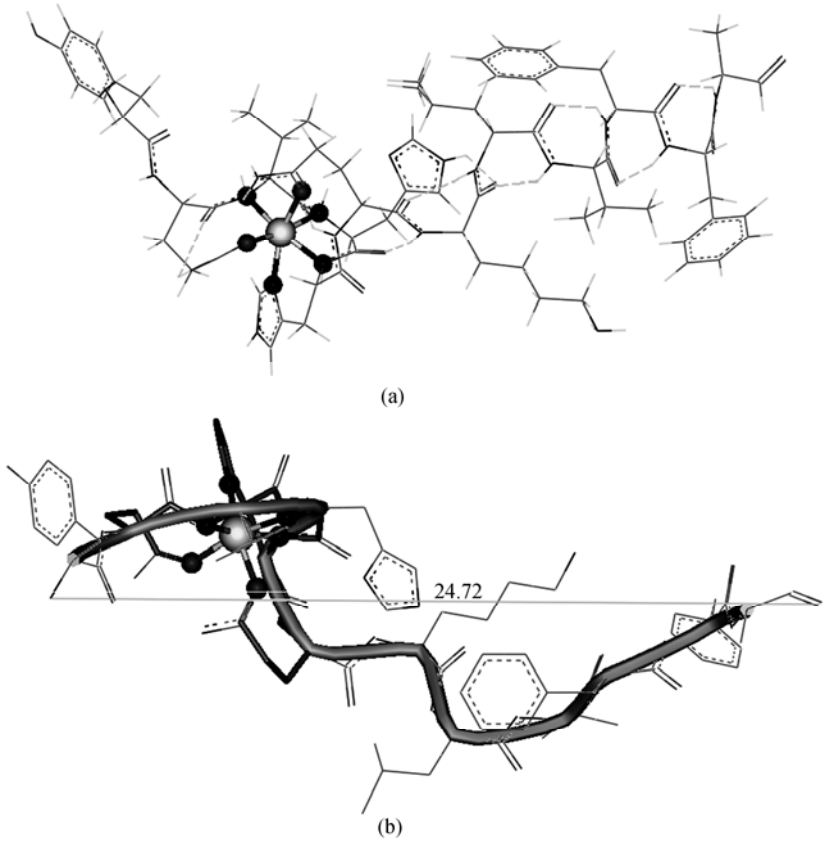

Fig. 6. Formation of intramolecular hydrogen bonds and its shrinkage effect. (a) Formation of intramolecular hydrogen bonds in [Cu-3N-Q15(O)-E11(O1)] complex; (b) the shrinkage effect of hydrogen bonds: the length of peptide chain shrank from 3.822 to 2.472 nm (24.72 in angstrom was the datum given by the software).

respectively. The energy contributions of two types of driving forces and the impact of two types of conformations on the aggregation were compared based on the calculations of system energies, respectively (see Fig. 6).

Table 6 Energy contributions of different interactions on aggregating system of double strands (kJ/mol)[a)]

	H-bond	Van der Waals
Standard Aβ	–72.6695	–26.5154
Distorted Aβ	+2.4607	+17.7552
Increased energy value	+75.1302	+44.2706

a) The potential of single Aβof standard βconformations and the potential of single Aβof distorted βconformations are regarded as reference value, respectively.

Fig. 6 shows that the hydrogen bonds interaction of backbones is the predominant driving force on the aggregation of standard Aβ. The contribution of hydrogen bonds on the stability of Aβ aggregation is near three times that of van der Waals interaction. The impact of structural distortion on hydrogen bonds is stronger than that on van der Waals interaction. The energy increase of Aβ aggregation due to losing of hydrogen bonds is near twice that due to losing of van der Waals interaction, i.e. structural distortion mainly destroys hydrogen bonds. The penta-ring complex [Cu-3N-Q15(O)-E11(O1)] with distorted conformation destroys the forming conditions of hydrogen bonds and weakens van der Waals interaction. So it is the increase of system energy and decline of stability that destroy and prohibit the aggregation.

(ii) The stability of aggregating systems. Using three kinds of monomers, i.e. [Cu-3N-Q15(O)-E11(O1)] complex with distorted β conformation, [Cu-H13(Nπ)-Y10(OH)] complex with local quasi-3.0_{10}-helix conformation and Aβ with standard parallel β conformation, two types of fibrils consisting of four and sixteen monomers were built agreeing with

the parameters of Lynn's structural model, respectively. Then the optimization of the system energies for the six kinds of fibrils was performed (see Tables 7 and 8).

Table 7 Comparison of the stabilities of aggregating system (kJ/mol)[a)]

Strands Number	Energy of Standard β	Energy of Distorted β	Increased energy Value of Distorted β
4	−177.9997	+46.5264	+224.5261
16	−1206.1342	+278.7467	+1484.8809

a) The potential of single Aβ of standard β conformations and that of distorted β conformations were regarded as reference value, respectively.

Table 8 Comparison of the stabilities of aggregating system (kJ/mol)[a)]

Strands Number	Energy of Standard β*	Energy of Quasi-3.0_{10}-helix	Increased energy Value of quasi-3.0_{10}-helix
4	−177.9997	+39.5474	+217.5471
16	−1206.1342	+230.2448	+1436.3790

a) The potential of single strand Aβ of standard β conformation and that of quasi-3.0_{10}-helix conformation were regarded as reference value, respectively.

The data in Tables 7 and 8 show that the energy trends of fibrils consisting of standard Aβ and distorted Aβ are oppositional with the increase of the number of monomers in fibrils. The energy of fibrils consisting of standard Aβ is much lower, yet the energy of fibrils consisting of distorted Aβ is much higher. The energy difference between fibrils consisting of standard Aβ and those consisting of distorted Aβ of [Cu-3N-Q15(O)-E11(O1)] complex is from 224.5261 to 1484.8809 kJ/mol with the increase of the number of monomers from four to sixteen. The energy difference between fibrils consisting of standard Aβ and those consisting of local quasi-3.0_{10}-helix Aβ of [Cu-H13(Nπ)-Y10(OH)] complex is from 217.5471 to 1436.3790 kJ/mol with the increase of the number of monomers from four to sixteen. All above indicate that the binding of Cu(II) with Aβ makes the conformation of Aβ transform from normal β conformation to "soluble conformations". The fibrils consisting of sixteen monomers of soluble conformation are associated by less hydrogen bonds and weaker van der Walls interaction, which results in the marked increase of system energy and significant decrease of stability. In sum, soluble conformations prefer the soluble forms rather than the insoluble form of aggregation in solution.

3 Conclusion

Investigation of the effects of metal ions on the aggregation of human Aβ is an inspiring and challenging task tightly related to the pathogenesis of AD[19]. The study of Zn(II)-induced Aβ aggregation elucidated that the interaction of Zn(II) with Aβ induces and enhances β-pleated conformation, and the binding of Zn(II) with Nτ is a common mode to stabilize the aggregating system. It may be reasonable to infer that the breakage of the Zn(II)-Nτ bond leads to the recovery of the Aβ solubility[6]. As the potential inhibitor of Zn(II) *in vivo*, Cu(II) interacts on Aβ by intramolecular chelation mode which induces local helix or random coil conformations and produces stably soluble complex. The possible inhibitory mechanism of copper(II) on Aβ aggregation was examined systematically by molecular modeling method in this work. Many questions unclear in the experimental studies, such as the soluble binding mode of [Cu(II)-Aβ] complex, the detailed coordinating microenvironment of typically soluble complexes, the conformational transition effect of Cu(II) and its impact on the stability of aggregation, were investigated. All results from this work will provide helpful clues for an improved understanding of the role of Cu(II) in the pathogenesis of AD and contribute to the development of an "anti-amyloid" therapeutic strategy.

Acknowledgements This work was supported by the National Natural Science Foundation of China (Grant No. 30470408).

References

1. Bush, A. I., Pettingell, W. H., Multhaup, G. et al., Rapid induction of Alzheimer Aβ amyloid formation by zinc, Science, 1994, 265: 1464—1467.
2. Frederickson, C. J., klitenick, M. A., Manton, W. I. et al., Cytoarchitectonic distribution of zinc in the hippocampus of man and the rat, Brain Res., 1983, 273: 335—339.
3. Waggoner, D. J., Drisaldi, B., Bartnikas, T. B. et al., Brain copper content and cuproenzyme activity do not vary with prion protein expression level, J. Biol. Chem., 2000, 275: 7455—7458.
4. Selkoe, D. J., Abraham, C. R., Podlisny, M. B. et al., Isolation of low-molecular-weight proteins from amyloid plaque fibers in Alzheimer's disease, J. Neurochem., 1986, 46: 1820—1834.
5. Storey, E., Cappai, R., The amyloid precursor protein of Alzheimer's disease and the Aβ peptide, Neuropathology and Applied Neurobiology, 1999, 25: 81—97.
6. Han Daxiong, Yang Pin, Molecular modeling on Zn(II) binding

modes of Alzheimer's amyloid β-peptide in insoluble aggregates and soluble complexes, Science in China, Series B (in Chinese), 2004, 48(2): 126—133.
7. Jin Zou, Kajita, K., Sugimoto, N., Cu^{2+} inhibits the aggregation of amyloid β-peptide(1–42) *in vitro*, Angew. Chem. Int. Ed., 2001, 40: 2274—2277.
8. Suzuki, K., Miura, T., Takeuchi, H., Inhibitory effect of copper(II) on zinc-induced aggregation of amyloid β-peptide, Biochem. Biophys. Res. Commun., 2001, 285: 991—996.
9. Burkoth, T. S., Benzinger, T. L. S., Urban, V. et al., Structure of the β-amyloid$_{(10–35)}$ fibril, J. Am. Chem. Soc., 2000, 122: 7883—7889.
10. Sunde, M., Blake, C. C. F., From the globular to the fibrous state: protein structure and structural conversion in amyloid formation, Q. Rev. Biophys., 1998, 31: 1—39.
11. Jian Dong, Atwood, C. S., Anderson, V. E. et al., Metal binding and oxidation of amyloid β within isolated senile plaque cores: Raman microscopic evidence, Biochemistry, 2003, 42: 2768—2773.
12. Morgan, D. M., Dong Jijun, Lynn, D. G., Metal switch for amyloid formation: insight into the structure of the nucleus, J. Am. Chem. Soc., 2002, 124: 12644—12645.
13. Sigel, H., Martin, R. B., Coordinating properties of the amide bond: Stability and structure of metal ion complexes of peptide and related ligands, Chem. Rev., 1982, 82: 385—426.
14. Sundberg, R. J., Martin, R. B., Interactions of histidine and other imidazole derivatives with transition metal ions in chemical and biological sytems, Chem. Rev., 1974, 74: 471—517.
15. Ciardelli, F., Tsuchida, E., Woehrle, D., Macromolecule-metal Complexes, Berlin, Heidelberg: Springer-Verlag, 1996, 130—151.
16. Miura, T., Suzuki, K., Kohata, N. et al., Metal binding mode of Alzheimer's amyloid β-peptide in insoluble aggregates and soluble complexes, Biochemistry, 2000, 39: 7024—7031.
17. Miura, T., Suzuki, K., Takeuchi, H., Binding of iron(III) to the single tyrosine residue of amyloid β-peptide probed by Raman spectroscopy, J. Molecular Structure, 2001, 598: 79—84.
18. Sigel, H., Martin, R. B., Coordinating properties of the amide bond: Stability and structure of metal ion complexes of peptide and related ligands, Chem. Rev., 1982, 82: 385—426.
19. Bush, A. I., Metals and neuroscience, Cur. Opin. Chem. Biol., 2000, 4: 184—191.